Emergence of topological defects and spin liquid in a two-orbital spin-fermion model on the honeycomb lattice

Kaidi Xu [1] Shan-Shan Wang [1,*] Rong Yu [2,3,†] and Shuai Dong [1,‡]

[1]*Key Laboratory of Quantum Materials and Devices of Ministry of Education, School of Physics,*
Southeast University, Nanjing 211189, China

[2]*School of Physics and Beijing Key Laboratory of Opto-electronic Functional Materials and Micro-nano Devices,*
Renmin University of China, Beijing 100872, China

[3]*Key Laboratory of Quantum State Construction and Manipulation (Ministry of Education), Renmin University of China,*
Beijing 100872, China

Stabilizing exotic quantum phases of matter, e.g., spin liquid, is an attractive topic in condensed matter. Here, by a Monte Carlo study of a two-orbital spin-fermion model on a honeycomb lattice, we show that the cooperative effects of the orbital degeneracy of itinerant electrons and the exchange interaction of localized spins can significantly suppress both ferromagnetic and antiferromagnetic orders by generating topological defects, and give rise to an intermediate spin-liquid state via continuous phase transitions. This phase competition can also be achieved by tuning the electron filling. These results shed light on realizing spin liquids on geometrically nonfrustrated lattices.

I. INTRODUCTION

The search for exotic magnetically disordered ground states, including both classical and quantum spin liquids (SLs) [1–5], is an ongoing theme in the condensed matter community, and tremendous progress has been made in frustrated spin systems [6,7]. However, besides several well-known examples, such as the Kitaev model on the honeycomb lattice [8], SL states in microscopic spin models relevant to real materials are yet to be justified. Meanwhile, this motivates another route in searching for SLs—by examining strongly correlated systems with itinerant electrons, for example, in Hubbard models in proximity to the Mott transition, or periodic Anderson models in certain limits [9–14]. Along this line, efforts have been made by considering systems with multiple orbitals and higher SU(N) ($N > 2$) symmetries [15–21].

Although appealing, including itinerant electrons in the model poses great challenges for unbiased numerical studies: Quantum Monte Carlo (MC) simulations would suffer a severe sign problem [22] when fermions of the system are away from half filling and density matrix renormalization group and/or tensor network methods are limited by the rapid increase of entanglement entropy of systems in spatial dimensions higher than one [23]. Consequently, the stabilization of SLs in these systems remains under debate [24–33], which motivates us to further look for the key ingredients to realizing these highly nontrivial states of matter in models with coupling between localized magnetic moments and itinerant electrons.

The Kondo lattice model (KLM) provides the simplest picture for describing the interplay between itinerant electrons and local magnetic moments [34–39]. In recent years, SL phases in KLM have been proposed, which have attracted a lot of attention [40–46]. The competition between Kondo screening and magnetic correlations mediated by the Ruderman-Kittel-Kasuya-Yosida (RKKY) interactions serves as an additional source of quantum fluctuations that may cause deconfinement of spinons, novel quantum criticality, and non-Fermi-liquid behavior [47–54]. With including the orbital degree of freedom, there are several well-established results that suggest orbital degeneracy may play a role similar to spin frustration and give rise to possible fractionalized Fermi liquids [49] and SL-like behavior [46]. Even when treating the local magnetic moments classically, highly nontrivial magnetic states can emerge, including a spiral antiferromagnet, skyrmion lattice (SkX) [55], as well as a disordered cooperative paramagnet [56].

In this paper, we consider a reduced form of the Kondo-Heisenberg model by taking the local moments as classical spins, which is often referred to as the spin-fermion model [57–60]. By studying a two-orbital spin-fermion model on a honeycomb lattice (see Fig. 1), we show the interplay between the orbital degeneracy of itinerant electrons and the antiferromagnetic (AFM) superexchange between neighboring spins can significantly suppress long-range magnetic orders by inducing various topological defects (TDs), driving the system into a SL state via continuous phase transitions. Remarkably, the SL state is stabilized within a certain regime of the phase diagram by tuning with either exchange coupling or electron filling. Our results suggest another route in realizing SLs in correlated multiorbital systems on geometrically nonfrustrated lattices.

*Contact author: wangss@seu.edu.cn
†Contact author: rong.yu@ruc.edu.cn
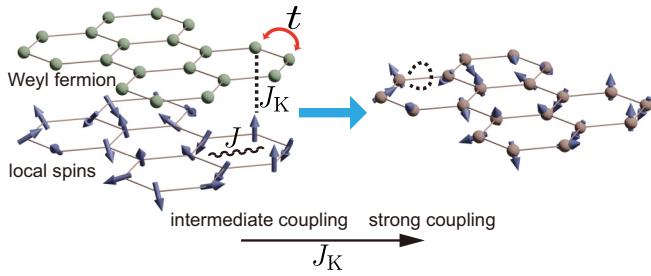‡Contact author: sdong@seu.edu.cn

FIG. 1. Sketch of the two-orbital spin-fermion model on a bilayer honeycomb lattice. Itinerant electrons described by a two-orbital Weyl semimetal model reside on the top layer of the lattice, with the hopping amplitude t. They are coupled to local spins (the bottom layer) via a ferromagnetic Kondo coupling J_K. In the strong-coupling limit ($|J_K| \gg |t|$), spins of itinerant electrons are aligned by local spins and their hopping integrals are renormalized by an emergent Berry phase Ω_{ij} at each bond. The neighboring spins are coupled with antiferromagnetic J.

II. MODEL AND METHOD

The Hamiltonian of the spin-fermion model we consider in this work reads as

$$H = \sum_{\langle ij \rangle \sigma}^{o,o'=\{a,b\}} t_{ij}^{oo'} c_{io\sigma}^\dagger c_{jo'\sigma} + J_K \sum_{i\alpha\beta}^{o} c_{io\alpha}^\dagger \sigma_{\alpha\beta} c_{io\beta} \cdot \mathbf{S}_i$$
$$+ J \sum_{\langle ij \rangle} \mathbf{S}_i \cdot \mathbf{S}_j + A_z \sum_i \left(S_i^z \right)^2, \tag{1}$$

where $c_{io\sigma}^\dagger$ creates an itinerant electron in orbital o with spin σ at site i of a honeycomb lattice. We consider a two-orbital model whose band structure describes a Weyl semimetal, and values of the nearest-neighboring hopping parameters $t_{ij}^{oo'}$ of this model can be found in Ref. [61]. $\mathbf{S}_i$ is the local spin operator, which is treated here as a classical $O(3)$ vector. J refers to the Heisenberg antiferromagnetic superexchange, and $A_z < 0$ refers to an easy-axis single-ion anisotropy. $J_K < 0$ is a ferromagnetic Kondo coupling. As a generally accepted approximation, $|J_K| \gg |t|$, then the spin of the itinerant electron is enforced to be in parallel to the local spin at that site. This leads to renormalization of the hopping integral $\tilde{t}_{ij}^{oo'} = \Omega_{ij} t_{ij}^{oo'}$ by a bond-dependent Berry phase Ω_{ij}, which is detailed in the Supplemental Material (SM) [62].

The Hamiltonian in Eq. (1) can be solved by combining MC and exact diagonalization techniques [60,61]. Within a fixed classical spin configuration $H(\{S_i\})$, it can be represented by a $2N \times 2N$ matrix where the fermion degree of freedom can be easily traced out by direct diagonalization by a standard library routine. After this procedure, the effective action is left purely classical and then the spin configuration can be stochastically sampled by Metropolis algorithms. During every MC evaluation, the diagonalization is performed beforehand. In the numerical calculation, we take one hopping parameter $t^{bb2} = 1$ as the energy scale. MC simulations are performed on lattices with a linear dimension from $L = 6$ to $L = 16$ (total number of sites $N = 2L^2$), with periodic boundary conditions.
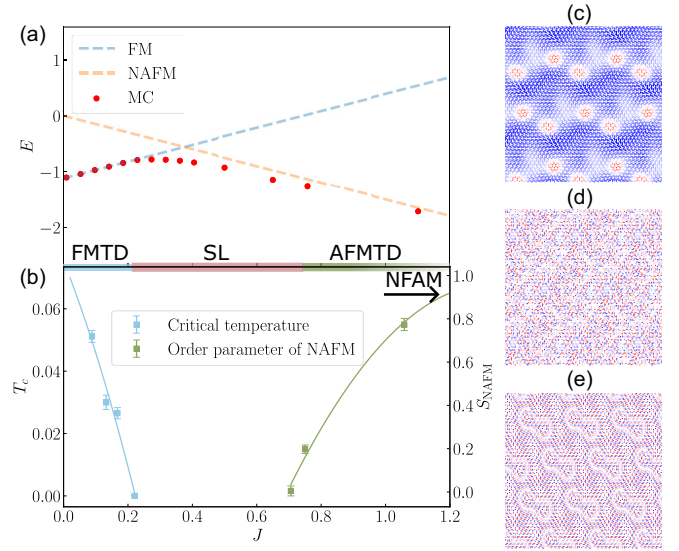

FIG. 2. (a) Evolution of the total energy E as a function of superexchange coupling J at quarter filling at (near) zero temperature. Dots: from MC simulations at extremely low temperature ($T = 0.002$). Dashed lines: for perfect FM and NAFM orders at $T = 0$. (b) The corresponding magnetic ground state phase diagram, determined from the evolution of FM T_C and the normalized static spin structure factor of the NAFM state. By increasing J, the ground state experiences a series of continuous phase transitions from the FM state first to a SL, then to a NAFM state. In either the FM or the NAFM phase, when close to the transition point to the SL phase, topological defects (TDs) of spin textures emerge which disturb the corresponding magnetic order. (c)–(e) Typical MC snapshots of spin textures at $T = 0.002$, in the FM ($J = 0.15$), SL ($J = 0.50$), and NAFM ($J = 1.12$) regions, respectively. In (c) the TDs are skyrmion-antiskyrmion pairs, and in (e) they form antiferromagnetic skyrmion-antiskyrmion pairs.

III. RESULTS

A. Evolution of magnetic phases at quarter filling

First, the evolution of magnetic ground states at quarter filling is studied by varying the superexchange coupling J. As shown in Fig. 2, for small J the ground state has a ferromagnetic (FM) order. As effects of the single-ion anisotropy, all spins are aligned along the S^z direction. The Curie temperature T_C of FM phase decreases with increasing J and becomes vanishingly small at $J \approx 0.22$. Above $J \approx 0.7$, the ground state develops a Néel AFM (NAFM) order, as demonstrated in Fig. 2(b) by the the inflection point of the static spin structure factor $S(\mathbf{q})$ at the NAFM wave vector $\mathbf{q} = (\pi, \pi)$ [62].

Second, for $0.22 \lesssim J \lesssim 0.7$, the spins do not show any feature in either the real-space pattern [Fig. 2(d)] or the structure factor in the momentum space [inset of Fig. 3(d)]. Moreover, our MC simulations do not find any spin freezing at low temperatures (see Fig. S2 in SM [62]). This, together with properties discussed below, suggests the magnetically disordered ground state in this intermediate J regime is a classical SL (sometimes also called a cooperative paramagnet [63]).

As shown in Fig. 3(a), in the zero-temperature limit, the total energy E and its first derivative dE/dJ vary continuously across the FM-to-SL transition, but the second derivative d^2E/dJ^2 exhibits a prominent peak. This implies that the
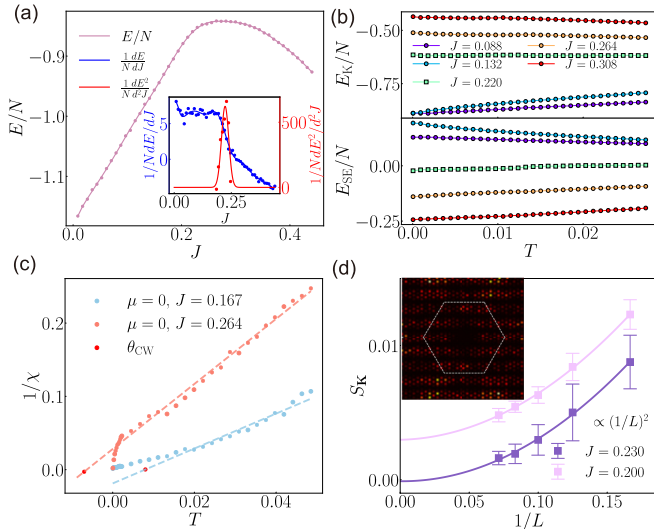
FIG. 3. (a) Evolution of the total energy E with J near the FM-to-SL transition. Inset: dE/dJ and d^2E/dJ^2. Both E and dE/dJ vary continuously while d^2E/dJ^2 exhibits a peak at $J = 0.22$, implying a second-order transition. (b) Temperature evolution of the kinetic energy E_K and the superexchange energy E_{SE} for selected J's. (c) Inverse of spin susceptibility $1/\chi$ as a function of temperature for the FM and SL ground states. Lines are the Curie-Weiss fits to high-temperature data. (d) Finite-size scaling of the spin structure factor at $\mathbf{q} = (0, 0)$ for two J's stabilizing the FM and SL ground states. Curves are quadratic fits. Inset: The static structure factor in the momentum space for $J = 0.230$.

FM-to-SL transition is second order. A similar conclusion applies to the SL-to-NAFM transition. Note that the nature of these transitions is in sharp contrast to that in one-orbital spin-fermion models on geometrically nonfrustrated lattices, in which tuning the superexchange coupling J usually induces a strong first-order transition between a FM metal and an insulating NAFM state [60,64,65]. It is rather similar to the (A)FM-to-SL transition in a frustrated lattice [56,66], although our system is nonfrustrated.

B. Topological defects and properties of SL

To better understand these magnetic transitions in our model, we examine the MC snapshots in FM and NAFM states. Remarkably, we find the real-space spin patterns close to the transitions contain various TDs. In the FM phase, depending on the value of J, they can be either skyrmion-antiskyrmion pairs, meron-antimeron pairs, vortex-antivortex pairs, or even their combinations, as shown in Fig. 2(c) and Fig. S2 in SM [62]. In the NAFM phase, TDs also appear in pairs, as illustrated in Fig. 2(e). The only difference is that spins on the two sublattices form interpenetrating skyrmions (or other TDs) with opposite chirality (referred to as an AFM skyrmion here). In both the FM and NAFM phases, TDs always appear in pairs, and each pair is formed by bounding one particle (skyrmion, meron, etc.) and its antiparticle counterpart with opposite chirality.

Recently, magnetic phases with nontrivial topological structures, such as a skyrmion crystal (SkX), have been extensively studied. A well-known mechanism to stabilize

these phases lies in the interplay between the Dzyaloshinskii-Moriya interaction, geometric/exchange frustration, and magnetic anisotropy [67]. It is also noticed that in centrosymmetric KLM, Fermi-surface nesting and an out-of-plane external field also play crucial roles [68,69]. The TDs emerging in our model are different from these known phases. Although the periodic structure of TDs cannot be fully excluded due to the small lattice used in simulation, the pairwise appearance of the TDs and the monotonically reduced but nonzero T_C imply that they are topological excitations disturbing the magnetic orders. The emergence of TDs provides a likely scenario for the FM(NAFM)-to-SL transition, i.e., the SL phase arises from a proliferation of TDs. Note here the easy-axis magnetic anisotropy excludes a Kosterlitz-Thouless (KT) transition. It would be then interesting to examine the universality of this transition.

It should be noted that the possible influence from a finite-size lattice is checked via scaling [Fig. 3(d)]. In addition, using a similar model [70], Matsui et al. proved that the size of the topological defects depends on the lifetime of the itinerant electrons and the coupling constant between electrons and localized spins, which are fixed in our simulation. Indeed, we did not find any evidence that the topological defects are unstable against the lattice size. Furthermore, by employing a one-orbital model which allows much larger lattices, the topological defects remain robust (Fig. S4 in SM) [62].

We then investigate the properties of the SL phase. Figure 3(b) shows the temperature dependence of the kinetic and superexchange energies (E_K and E_{SE}) per site at several J values. For the FM phase, both energies show clear temperature dependence. Near the critical point $J = 0.22$, both energies show minimal temperature dependence. Further increasing J where the ground state becomes a SL, the temperature dependence of both energies remains weak. Note that the entropy is evaluated by the integration of $1/T \, dE/dT$, and the weak temperature dependence of energies suggests a large residual entropy of the SL. Also note that compared to E_{SE}, E_K shows an even weaker temperature dependence in the SL phase. This implies that the residual entropy is mainly ascribed to the orbital fluctuations of the model, given that the lattice has no geometric frustration. This is in contrast to the case with geometric frustration [56] where both E_K and E_{SE} show minimum temperature dependence only within a narrow critical regime.

We now turn to study the temperature dependence of the magnetic susceptibility χ, which usually follows a Curie-Weiss behavior at high temperatures as $\chi = C/(T - \theta_{CW})$, where C is a constant and θ_{CW} is the Curie-Weiss temperature. The Curie-Weiss fit provides not only an estimate of the exchange interaction but also a measurement of frustration. Figure 3(c) shows the $1/\chi$ for two J values below and above the FM-to-SL transition, respectively. For $J = 0.167$ (in the FM region), the fitted Curie-Weiss temperature $\theta_{CW} \approx 0.01$, indicating an effective FM interaction among spins. Moreover, $1/\chi$ deviates from the Curie-Weiss behavior at $T \approx 0.02$. This temperature is slightly higher than θ_{CW}, indicating a rather weak frustration effect for this J. In contrast, for $J = 0.264$ (in the SL region), the fitted $\theta_{CW} \approx -0.01$, showing that the effective exchange interaction changes to AFM. Interestingly, for $T \ll |\theta_{CW}|$, χ undergoes a Curie crossover to $1/\chi \sim T$
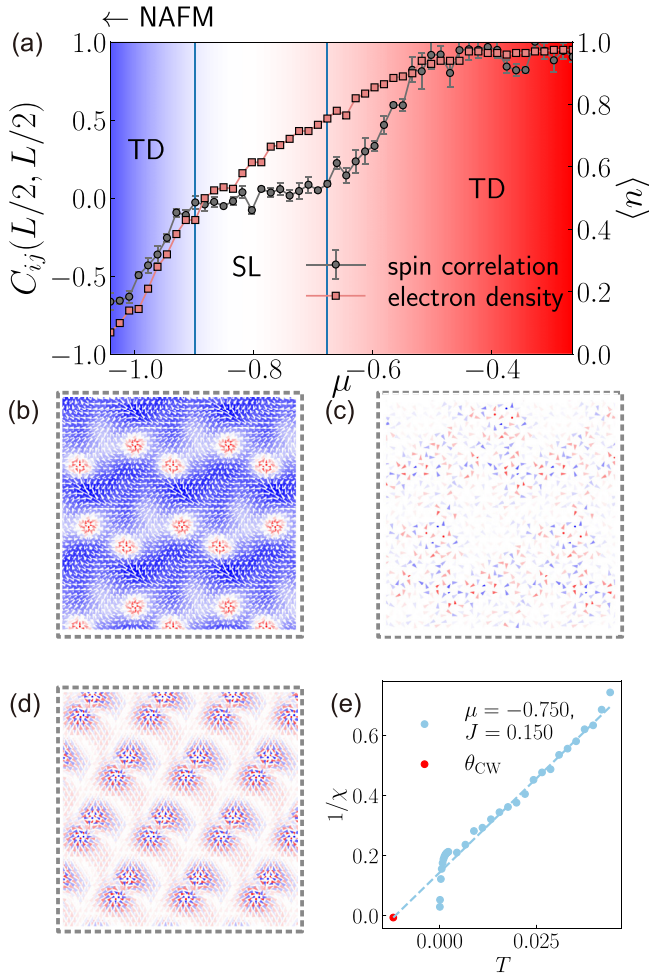
FIG. 4. The phase diagram as a function of chemical potential with fixed $J = 0.15$ and at $T = 0.002$. The squares represent the density of itinerant electrons per site while the circles represent the real-space correlation function. (b)–(d) The MC snapshots for $\mu = -0.95, -0.8$, and -0.5, respectively. (e) The inverse susceptibility for $\mu = -0.75$.

behavior. Such a crossover behavior indicates strong spin frustration and has been observed in a number of SL models [71] and SL candidate materials [72]. In addition, the finite-size scaling analysis in Fig. 3(d) indicates that within this SL regime, the magnetic order parameter drops to zero in the thermodynamic limit, confirming that the system is magnetically disordered.

IV. DISCUSSION

Besides the superexchange coupling J, the FM-SL-AFM transition can also be induced by tuning the chemical potential μ. Figure 4 shows a typical phase diagram of the system with μ for $J = 0.15$. To trace the variation of magnetic order with μ, we calculate the spin correlation function $C(\mathbf{R}) = \langle \mathbf{S}_i \cdot \mathbf{S}_{i+\mathbf{R}} \rangle$ at the largest spatial distance $\mathbf{R} = (L/2, L/2)$. At quarter filling (i.e., electron density per site $\langle n \rangle = 1$), the ground state is FM [i.e., $C(\mathbf{R}) \approx 1$]. With decreasing μ, the electron density decreases continuously, and TDs appear [see Fig. 4(b)]. For $\langle n \rangle \lesssim 0.8$, $C(\mathbf{R})$ develops a zero plateau, indicating the suppression of the FM order and the emergence

of the SL. This SL phase is stabilized until $\langle n \rangle \approx 0.5$ (1/8 filling). In analogy to the quarter-filling case, this SL exhibits a disordered spin pattern [Fig. 4(c)] and a Curie crossover in the susceptibility [Fig. 4(e)].

Further decreasing the chemical potential yields the NAFM phase, as characterized by a negative $C(\mathbf{R})$. Interestingly, AFM TDs are observed in the NAFM phase, as shown in Fig. 4(d). Stabilization of the SL within a finite range of electron filling suggests that this phase is insensitive to the shape of the Fermi surface, which is known to be relevant for weak Kondo couplings [55]. In our case, the SL phase instead emerges as a compromise of the competing FM double-exchange and AFM superexchange interactions. In the vicinity of the SL phase, TDs appear as a consequence of strong fluctuations induced by this competition, which are further enhanced by the nontrivial topology of the band structure.

As a final remark, it has been known that an intermediate regime for SL phase in the one-orbital Dirac fermion model does not exist, even if the correlation effect is considered [29,73], namely the electron correlation alone is not enough in searching for such a highly entangled state of matter. Then it is of great interest to examine whether the degenerate orbitals can introduce another flavor of gauge field fluctuation, a defining characteristic of a SL. Here, a two-orbital basis on the honeycomb lattice has been tested, which naturally manifests a Weyl-type band structure in the reciprocal space. In the spin-fermion model (one-orbital or two-orbital), the exchange frustration from antiferromagnetic J can naturally tune the ground state from ferromagnetism to antiferromagnetism, with topological defects in real space emerging during this transition. The most interesting physics is that only in the two-orbital version the SL phase can survive as an intermediate phase, in which the orbital degeneracy plays the essential role. This scenario is summarized in Fig. S3 in SM, and the controlled study of the one-orbital model can be found in Fig. S4 in SM [62].

V. CONCLUSION

To summarize, in our model, topological defects have been observed in both ferromagnetic and antiferromagnetic phases in a two-orbital spin-fermion model on the honeycomb lattice. These topological defects suppress magnetic orders and eventually lead to an intermediate spin-liquid phase via continuous quantum phase transitions, which can be achieved by tuning either the superexchange interaction or the electron density. Our results suggest that fluctuations introduced by orbital degeneracy can be a possible recipe for preparing a highly nontrivial quantum state on a geometrically nonfrustrated lattice. The model proposed here has the potential to be realized in the recently discovered itinerant magnetic materials on the hexagonal lattice with a partially filled e_g manifold [74], dilute honeycomb magnets [75], or an ultracold atomic optical lattice which can mimic the SU(N) ($N \geqslant 2$) double-exchange model [76].

[1] P. W. Anderson, Resonating valence bonds: A new kind of insulator? Mater. Res. Bull. **8**, 153 (1973).

[2] C. Broholm, R. J. Cava, S. A. Kivelson, D. G. Nocera, M. R. Norman, and T. Senthil, Quantum spin liquids, Science **367**, eaay0668 (2020).

[3] L. Balents, Spin liquids in frustrated magnets, Nature (London) **464**, 199 (2010).

[4] L. Savary and L. Balents, Quantum spin liquids: a review, Rep. Prog. Phys. **80**, 016502 (2017).

[5] M. Udagawa and L. D. C. Jaubert, *Spin Ice* (Springer, Berlin, 2021).

[6] H. T. Diep, *Frustrated Spin Systems* (World Scientific, Singapore, 2005).

[7] *Introduction to Frustrated Magnetism: Materials, Experiments, Theory*, edited by C. Lacroix, P. Mendels, and F. Mila, Springer Series in Solid-State Science, Vol. 164 (Springer, Berlin, 2011).

[8] A. Kitaev, Anyons in an exactly solved model and beyond, Ann. Phys. **321**, 2 (2006).

[9] L. Balents, L. Bartosch, A. Burkov, S. Sachdev, and K. Sengupta, Putting competing orders in their place near the Mott transition, Phys. Rev. B **71**, 144508 (2005).

[10] T. Senthil, Theory of a continuous Mott transition in two dimensions, Phys. Rev. B **78**, 045109 (2008).

[11] D. Podolsky, A. Paramekanti, Y. B. Kim, and T. Senthil, Mott transition between a spin-liquid insulator and a metal in three dimensions, Phys. Rev. Lett. **102**, 186401 (2009).

[12] T. Grover, N. Trivedi, T. Senthil, and P. A. Lee, Weak Mott insulators on the triangular lattice: Possibility of a gapless nematic quantum spin liquid, Phys. Rev. B **81**, 245121 (2010).

[13] S.-S. Lee and P. A. Lee, U(1) gauge theory of the Hubbard model: Spin liquid states and possible application to κ-(BEDT-TTF)$_2$Cu$_2$(CN)$_3$, Phys. Rev. Lett. **95**, 036403 (2005).

[14] P. Ribeiro and P. A. Lee, Magnetic impurity in a $U(1)$ spin liquid with a spinon Fermi surface, Phys. Rev. B **83**, 235119 (2011).

[15] E. Ibarra-García-Padilla, S. Dasgupta, H.-T. Wei, S. Taie, Y. Takahashi, R. T. Scalettar, and K. R. A. Hazzard, Universal thermodynamics of an SU(N) Fermi-Hubbard model, Phys. Rev. A **104**, 043316 (2021).

[16] X. Cao, Y. Lu, P. Hansmann, and M. W. Haverkort, Tree tensor-network real-time multiorbital impurity solver: Spin-orbit coupling and correlation functions in Sr$_2$RuO$_4$, Phys. Rev. B **104**, 115119 (2021).

[17] Z. Cheng and C. A. Marianetti, Precise ground state of multiorbital Mott systems via the variational discrete action theory, Phys. Rev. B **106**, 205129 (2022).

[18] J. E. Han, M. Jarrell, and D. L. Cox, Multiorbital Hubbard model in infinite dimensions: Quantum Monte Carlo calculation, Phys. Rev. B **58**, R4199(R) (1998).

[19] K. M. Stadler, Z. P. Yin, J. von Delft, G. Kotliar, and A. Weichselbaum, Dynamical mean-field theory plus numerical renormalization-group study of spin-orbital separation in a three-band hund metal, Phys. Rev. Lett. **115**, 136401 (2015).

[20] F. B. Kugler, M. Zingl, H. U. R. Strand, S.-S. B. Lee, J. von Delft, and A. Georges, Strongly correlated materials from a numerical renormalization group perspective: How the fermi-liquid state of Sr$_2$RuO$_4$ emerges, Phys. Rev. Lett. **124**, 016401 (2020).

[21] K. M. Stadler, G. Kotliar, A. Weichselbaum, and J. von Delft, Hundness versus Mottness in a three-band Hubbard–Hund model: On the origin of strong correlations in Hund metals, Ann. Phys. **405**, 365 (2019).

[22] M. Troyer and U.-J. Wiese, Computational complexity and fundamental limitations to fermionic quantum Monte Carlo simulations, Phys. Rev. Lett. **94**, 170201 (2005).

[23] J. I. Cirac, D. Pérez-García, N. Schuch, and F. Verstraete, Matrix product states and projected entangled pair states: Concepts, symmetries, theorems, Rev. Mod. Phys. **93**, 045003 (2021).

[24] Z. Y. Meng, T. C. Lang, S. Wessel, F. F. Assaad, and A. Muramatsu, Quantum spin liquid emerging in two-dimensional correlated Dirac fermions, Nature (London) **464**, 847 (2010).

[25] C.-C. Chang and R. T. Scalettar, Quantum disordered phase near the Mott transition in the staggered-flux Hubbard model on a square lattice, Phys. Rev. Lett. **109**, 026404 (2012).

[26] Q. Chen, G. H. Booth, S. Sharma, G. Knizia, and G. K.-L. Chan, Intermediate and spin-liquid phase of the half-filled honeycomb Hubbard model, Phys. Rev. B **89**, 165134 (2014).

[27] S. Sorella, Y. Otsuka, and S. Yunoki, Absence of a spin liquid phase in the Hubbard model on the honeycomb lattice, Sci. Rep. **2**, 992 (2012).

[28] S. R. Hassan and D. Sénéchal, Absence of spin liquid in non-frustrated correlated systems, Phys. Rev. Lett. **110**, 096402 (2013).

[29] Y. Otsuka, S. Yunoki, and S. Sorella, Universal quantum criticality in the metal-insulator transition of two-dimensional interacting Dirac electrons, Phys. Rev. X **6**, 011029 (2016).

[30] Y. Otsuka, K. Seki, S. Sorella, and S. Yunoki, Dirac electrons in the square-lattice Hubbard model with a d-wave pairing field: The chiral Heisenberg universality class revisited, Phys. Rev. B **102**, 235105 (2020).

[31] D. Ixert, F. F. Assaad, and K. P. Schmidt, Mott physics in the half-filled Hubbard model on a family of vortex-full square lattices, Phys. Rev. B **90**, 195133 (2014).

[32] F. Parisen Toldin, M. Hohenadler, F. F. Assaad, and I. F. Herbut, Fermionic quantum criticality in honeycomb and π-flux Hubbard models: Finite-size scaling of renormalization-group-invariant observables from quantum Monte Carlo, Phys. Rev. B **91**, 165108 (2015).

[33] F. F. Assaad and I. F. Herbut, Pinning the order: The nature of quantum criticality in the Hubbard model on honeycomb lattice, Phys. Rev. X **3**, 031010 (2013).

[34] J. Kondo, Resistance minimum in dilute magnetic alloys, Prog. Theor. Phys. **32**, 37 (1964).

[35] C. Zener, Interaction between the *d*-shells in the transition metals. II. Ferromagnetic compounds of manganese with perovskite structure, Phys. Rev. **82**, 403 (1951).

[36] P. W. Anderson and H. Hasegawa, Considerations on double exchange, Phys. Rev. **100**, 675 (1955).

[37] P. G. de Gennes, Effects of double exchange in magnetic crystals, Phys. Rev. **118**, 141 (1960).

[38] J. B. Goodenough, Theory of the role of covalence in the perovskite-type manganites [La, *M*(II)]MnO₃, Phys. Rev. **100**, 564 (1955).

[39] H.-H. Lai, S. E. Grefe, S. Paschen, and Q. Si, Weyl–Kondo semimetal in heavy-fermion systems, Proc. Natl. Acad. Sci. USA **115**, 93 (2018).

[40] P. Coleman and N. Andrei, Kondo-stabilised spin liquids and heavy fermion superconductivity, J. Phys.: Condens. Matter **1**, 4057 (1989).

[41] S. Burdin, D. R. Grempel, and A. Georges, Heavy-fermion and spin-liquid behavior in a Kondo lattice with magnetic frustration, Phys. Rev. B **66**, 045111 (2002).

[42] S. Florens, L. Fritz, and M. Vojta, Kondo effect in bosonic spin liquids, Phys. Rev. Lett. **96**, 036601 (2006).

[43] I. Paul, C. Pépin, and M. R. Norman, Kondo breakdown and hybridization fluctuations in the Kondo-Heisenberg lattice, Phys. Rev. Lett. **98**, 026402 (2007).

[44] J. Wang and Y.-F. Yang, $\mathbb{Z}_2$ metallic spin liquid on a frustrated Kondo lattice, Phys. Rev. B **106**, 115135 (2022).

[45] B. Bauer, B. P. Keller, S. Trebst, and A. W. W. Ludwig, Symmetry-protected non-Fermi liquids, kagome spin liquids, and the chiral Kondo lattice model, Phys. Rev. B **99**, 035155 (2019).

[46] K. P. Wójcik and J. Kroha, Quantum spin liquid in an RKKY-coupled two-impurity Kondo system, Phys. Rev. B **107**, L121111 (2023).

[47] X. G. Wen, Effective Lagrangian for holes in the spin-liquid state, Phys. Rev. B **39**, 7223 (1989).

[48] X. G. Wen, Mean-field theory of spin-liquid states with finite energy gap and topological orders, Phys. Rev. B **44**, 2664 (1991).

[49] T. Senthil, S. Sachdev, and M. Vojta, Fractionalized Fermi liquids, Phys. Rev. Lett. **90**, 216403 (2003).

[50] D. L. Cox and A. E. Ruckenstein, Spin-flavor separation and non-Fermi-liquid behavior in the multichannel Kondo problem: A large-*N* approach, Phys. Rev. Lett. **71**, 1613 (1993).

[51] U. F. P. Seifert, T. Meng, and M. Vojta, Fractionalized Fermi liquids and exotic superconductivity in the Kitaev-Kondo lattice, Phys. Rev. B **97**, 085118 (2018).

[52] A. Altland, B. Béri, R. Egger, and A. M. Tsvelik, Multichannel Kondo impurity dynamics in a Majorana device, Phys. Rev. Lett. **113**, 076401 (2014).

[53] N. Andrei and A. Jerez, Fermi- and non-Fermi-liquid behavior in the anisotropic multichannel Kondo model: Bethe ansatz solution, Phys. Rev. Lett. **74**, 4507 (1995).

[54] Y. Ge and Y. Komijani, Emergent spinon dispersion and symmetry breaking in two-channel Kondo lattices, Phys. Rev. Lett. **129**, 077202 (2022).

[55] Z. Wang, Y. Su, S.-Z. Lin, and C. D. Batista, Skyrmion crystal from RKKY interaction mediated by 2D electron gas, Phys. Rev. Lett. **124**, 207201 (2020).

[56] Y. Motome and N. Furukawa, Phase competition in the double-exchange model on the frustrated pyrochlore lattice, Phys. Rev. Lett. **104**, 106407 (2010).

[57] C. Buhler, S. Yunoki, and A. Moreo, Magnetic domains and stripes in a spin-fermion model for cuprates, Phys. Rev. Lett. **84**, 2690 (2000).

[58] S. Liang, G. Alvarez, C. Şen, A. Moreo, and E. Dagotto, Anisotropy of electrical transport in pnictide superconductors studied using Monte Carlo simulations of the spin-fermion model, Phys. Rev. Lett. **109**, 047001 (2012).

[59] A. Moreo, S. Yunoki, and E. Dagotto, Phase separation scenario for manganese oxides and related materials, Science **283**, 2034 (1999).

[60] S. Yunoki, J. Hu, A. L. Malvezzi, A. Moreo, N. Furukawa, and E. Dagotto, Phase separation in electronic models for manganites, Phys. Rev. Lett. **80**, 845 (1998).

[61] K. Xu, D. Hu, J. Chen, H. Ye, L. Han, S.-S. Wang, and S. Dong, Two-orbital spin-fermion model study of ferromagnetism in the honeycomb lattice, Phys. Rev. B **108**, 094401 (2023).

[62] See Supplemental Material at http://link.aps.org/supplemental/10.1103/PhysRevB.111.014413 for details of the Hamiltonian, numerical methods, and more results, which includes Refs. [29,60,61,73].

[63] R. Moessner and J. T. Chalker, Properties of a classical spin liquid: The Heisenberg pyrochlore antiferromagnet, Phys. Rev. Lett. **80**, 2929 (1998).

[64] S. Yunoki and A. Moreo, Static and dynamical properties of the ferromagnetic Kondo model with direct antiferromagnetic coupling between the localized t_{2g} electrons, Phys. Rev. B **58**, 6403 (1998).

[65] E. Dagotto, S. Yunoki, A. L. Malvezzi, A. Moreo, J. Hu, S. Capponi, D. Poilblanc, and N. Furukawa, Ferromagnetic Kondo model for manganites: Phase diagram, charge segregation, and influence of quantum localized spins, Phys. Rev. B **58**, 6414 (1998).

[66] J. Chaloupka, G. Jackeli, and G. Khaliullin, Zigzag magnetic order in the iridium oxide Na₂IrO₃, Phys. Rev. Lett. **110**, 097204 (2013).

[67] A. Fert, N. Reyren, and V. Cros, Magnetic skyrmions: advances in physics and potential applications, Nat. Rev. Mater. **2**, 17031 (2017).

[68] R. Ozawa, S. Hayami, and Y. Motome, Zero-field skyrmions with a high topological number in itinerant magnets, Phys. Rev. Lett. **118**, 147205 (2017).

[69] R. Eto, R. Pohle, and M. Mochizuki, Low-energy excitations of skyrmion crystals in a centrosymmetric Kondo-lattice magnet: Decoupled spin-charge excitations and nonreciprocity, Phys. Rev. Lett. **129**, 017201 (2022).

[70] A. Matsui, T. Nomoto, and R. Arita, Skyrmion-size dependence of the topological Hall effect: A real-space calculation, Phys. Rev. B **104**, 174432 (2021).

[71] R. Pohle and L. D. C. Jaubert, Curie-law crossover in spin liquids, Phys. Rev. B **108**, 024411 (2023).

[72] J. S. Helton, K. Matan, M. P. Shores, E. A. Nytko, B. M. Bartlett, Y. Yoshida, Y. Takano, A. Suslov, Y. Qiu, J.-H. Chung, D. G. Nocera, and Y. S. Lee, Spin dynamics of the spin-1/2 kagome lattice antiferromagnet ZnCu₃(OH)₆Cl₂, Phys. Rev. Lett. **98**, 107204 (2007).

[73] M. Qin, C.-M. Chung, H. Shi, E. Vitali, C. Hubig, U. Schollwöck, S. R. White, and S. Zhang, Absence of superconductivity in the pure two-dimensional Hubbard model, Phys. Rev. X **10**, 031016 (2020).

[74] R. Takagi, J. S. White, S. Hayami, R. Arita, D. Honecker, H. M. Rønnow, Y. Tokura, and S. Seki, Multiple-q noncollinear magnetism in an itinerant hexagonal magnet, Sci. Adv. **4**, eaau3402 (2018).

[75] S. Lee, Y. S. Choi, S.-H. Do, W. Lee, C. H. Lee, M. Lee, M. Vojta, C. N. Wang, H. Luetkens, Z. Guguchia, and K.-Y. Choi, Kondo screening in a Majorana metal, Nat. Commun. **14**, 7405 (2023).

[76] A. V. Gorshkov, M. Hermele, V. Gurarie, C. Xu, P. S. Julienne, J. Ye, P. Zoller, E. Demler, M. D. Lukin, and A. M. Rey, Two-orbital $SU(N)$ magnetism with ultracold alkaline-earth atoms, Nat. Phys. **6**, 289 (2010).